Anatomy of the Inferior Orbital Fissure: Implications for Endoscopic Cranial Base Surgery

Juan Carlos De Battista, M.D. [1] Lee A. Zimmer, M.D. [1, 2] Philip V. Theodosopoulos, M.D. [1]
Sebastien C. Froelich, M.D., Ph.D. [1] Jeffrey T. Keller, Ph.D. [1, 3]

[1] Department of Neurosurgery, University of Cincinnati (UC) Neuroscience Institute, UC College of Medicine, Cincinnati, Ohio
[2] Department of Otolaryngology–Head and Neck Surgery, University of Cincinnati (UC) Neuroscience Institute, UC College of Medicine, Cincinnati, Ohio
[3] Mayfield Clinic, Cincinnati, Ohio

Address for correspondence and reprint requests Jeffrey T. Keller, Ph.D., Editorial Office, Department of Neurosurgery, ML 0515, University of Cincinnati College of Medicine, Cincinnati, OH 45267-0515 (e-mail: editor@mayfieldclinic.com).

J Neurol Surg B 2012;73:132–138.

Abstract

Considering many approaches to the skull base confront the inferior orbital fissure (IOF) or sphenomaxillary fissure, the authors examine this anatomy as an important endoscopic surgical landmark. In morphometric analyses of 50 adult human dry skulls from both sexes, we divided the length of the IOF into three segments (anterolateral, middle, posteromedial). Hemotoxylin- and eosin-stained sections were analyzed. Dissections were performed using transnasal endoscopy in four formalin-fixed cadaveric cranial specimens (eight sides); three endoscopic approaches to the IOF were performed. IOF length ranged from 25 to 35 mm (mean 29 mm). Length/width of the individual anterolateral, middle, and posteromedial segments averaged 6.46/5, 4.95/3.2, and 17.6/ 2.4 mm, respectively. Smooth muscle within the IOF had a consistent relationship with several important anatomical landmarks. The maxillary antrostomy, total ethmoidectomy approach allowed access to the posteromedial segment of the fissure. The endoscopic modified, medial maxillectomy approach allowed access to the middle and posterior-medial segment. The Caldwell-Luc approach allowed complete exposure of the IOF. The IOF serves as an important anatomic landmark during endonasal endoscopic approaches to the skull base and orbit. Each of the three segments provides a characteristic endoscopic corridor, unique to the orbit and different fossas surrounding the fissure.

Keywords
- skull base
- endoscope
- inferior orbital fissure
- orbit
- pterygopalatine fossa

The development of endonasal, endoscopic cranial base surgery has permitted access to the anterior and inferior aspects of the skull base using various surgical corridors.[1–12] Endoscopic transmaxillary, transethmoidal, and transsphenoidal approaches often rely on the collaboration between specialists in the fields of otolaryngology and neurosurgery. Many approaches to the skull base either confront or come in close proximity to the inferior orbital fissure (IOF). Nevertheless, the IOF (also called the sphenomaxillary fissure) has been neglected as an endoscopic surgical landmark.[4,5,8,13–21]

The IOF lies in the orbital floor in proximity to the superior orbital fissure (SOF), foramen rotundum, pterygopalatine fossa, infratemporal fossa, and temporal fossa. Because trauma, tumor, and/or infection can affect all of these structures or regions, understanding the anatomical detail of the IOF is essential.[22–27] Its anatomy was previously described in relation to an orbitozygomatic osteotomy,[28–31] yet its comprehensive three-dimensional (3D) anatomical relationships have not been described from an endoscopic perspective.

received
June 22, 2011
accepted after revision
October 11, 2011
published online
February 6, 2012

DOI http://dx.doi.org/10.1055/s-0032-1301398.
ISSN 2193-6331.

In this study, we describe the microanatomic and endoscopic detail of the IOF, utilizing a morphometric analysis of cadaveric dry skulls, endoscopic dissection of cadaveric specimens, and histological examination of the IOF and surrounding areas. Particular attention is focused on the IOF and its relationship to adjacent structures. An endoscopic classification of the IOF is presented that has clinical application and relevance during endoscopic skull base surgery.

Materials and Methods

Morphometric analysis of the IOF was completed in 50 adult human dry skulls (100 sides) of both sexes. The distance of the IOF from the anterior aspect of the maxillary strut to the most anterolateral aspect of the fissure was measured with calipers. The IOF was divided into three segments: (1) posteromedial, from the maxillary strut to the posterior border of the infraorbital groove; (2) middle, the width of the infraorbital groove or canal at the IOF; and (3) anterolateral, from the anterior border of the infraorbital groove or canal to the most anterolateral aspect of the IOF (►**Fig. 1**). For each segment, the width was measured in the posteromedial segment at the anterior or exocranial aspect of the maxillary strut, middle segment at the center of the infraorbital groove, and anterolateral segment at its anterior most aspect.

Histological sections of the human newborn head from the permanent collection of the Institute of Anatomy (University of Strasbourg, Strasbourg, France) were obtained from ectopic pregnancies or spontaneous abortions. Coronal sections (340 µm) of the entire head were stained with hematoxylin and eosin. Every 10th section was stained with Masson trichome to critically examine the region of the IOF.

Cadaveric studies of four formalin-fixed cranial specimens injected with colored latex were performed.[32] Standard instrumentation for endoscopic sinus surgery and 0-degree nasal endoscopes (Medtronic, Jacksonville, FL) was used. Images were recorded by a 1088 image capture device (Stryker, Kalamazoo, MI). Eight IOFs were dissected using three different corridors: total maxillary antrostomy and ethmoidectomy; an endoscopic-modified medial maxillectomy; and a combined endoscopic-modified medial maxillectomy and Caldwell-Luc approaches.

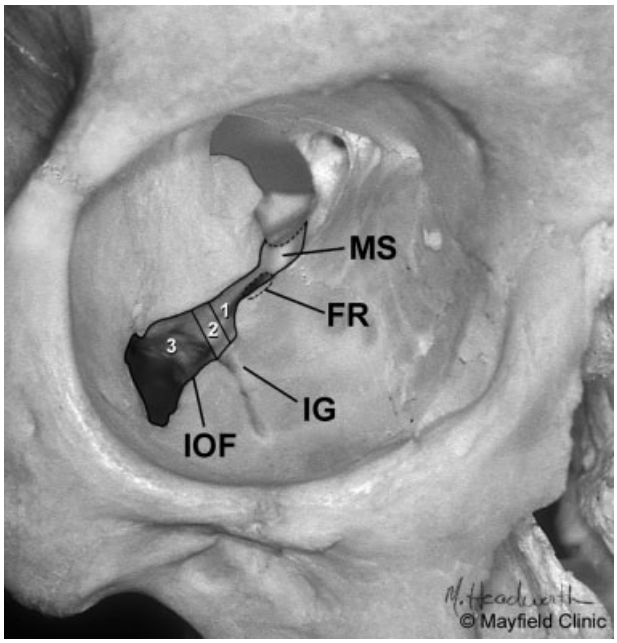

Figure 1 Photograph of the right orbit illustrates osseous structures, especially the three segments of the inferior orbital fissure (IOF). Posteromedial segment, from the maxillary strut (MS) to the posterior border of the infraorbital groove (IG). Middle segment, the width of the infraorbital groove or canal at the IOF. Anterolateral segment, from the anterior border of the IG or canal to the most anterolateral aspect of the IOF. (Printed with permission from Mayfield Clinic). FR, foramen rotundum.

Results

Morphometric Analysis

The IOF or sphenomaxillary fissure is defined as a space between the lateral wall and floor of the orbit. This fissure runs in an anterolateral direction from the maxillary strut posteriorly to the zygomatic bone anteriorly. The IOF joins the orbit with the pterygopalatine, infratemporal, and temporal fossae. Posterolaterally, the IOF is bounded by the lower margin of the orbital surface of the greater wing of the sphenoid, laterally by the zygoma, posteromedially by the orbital process of the palatine bone, and anteriorly by the maxilla. In the posteromedial segment, the foramen rotundum, superior orbital fissure, and pterygopalatine fossa communicate with the orbit and cavernous sinus, the middle segment of the IOF communicates with the infratemporal fossa whereas the anterolateral segment allows access to the temporal fossa (►**Fig. 2**). The IOF is narrower at its center and its long axis lies along the line between the zygomaticofacial foramen and optic canal.

►**Table 1** summarizes the measurements of length, width, and segments of the IOF. Length averaged 29.1 mm (range: 23 to 35 mm). Average lengths of the posteromedial, middle, and anterolateral segments were 17.0, 5.0, and 6.5, respectively. Average widths of the posteromedial, middle, and anterolateral segments were 2.4, 3.2, and 5 mm, respectively.

Histological Examination

Histological analysis confirmed the relationship of the IOF and the various fossae identified above (►**Fig. 3**). Smooth muscle was present filling the entire IOF in all specimens studied.[33] The superior aspect of this muscle has a direct relationship with orbital contents, especially the inferior rectus. Inferiorly, the muscle contributes to the roof of the pterygopalatine fossa and its contents including branches of the maxillary artery, rami of the maxillary nerve, and pterygopalatine ganglion. The zygomatic nerve courses within this muscle. Posteromedially, the muscle courses above the maxillary strut and inferiorly to the annulus of Zinn, via the medial and inferior aspect of the superior orbital fissure extending to the anterior venous confluence of the cavernous sinus. Anteriorly, this muscle spans the IOF from one bony margin to the other.

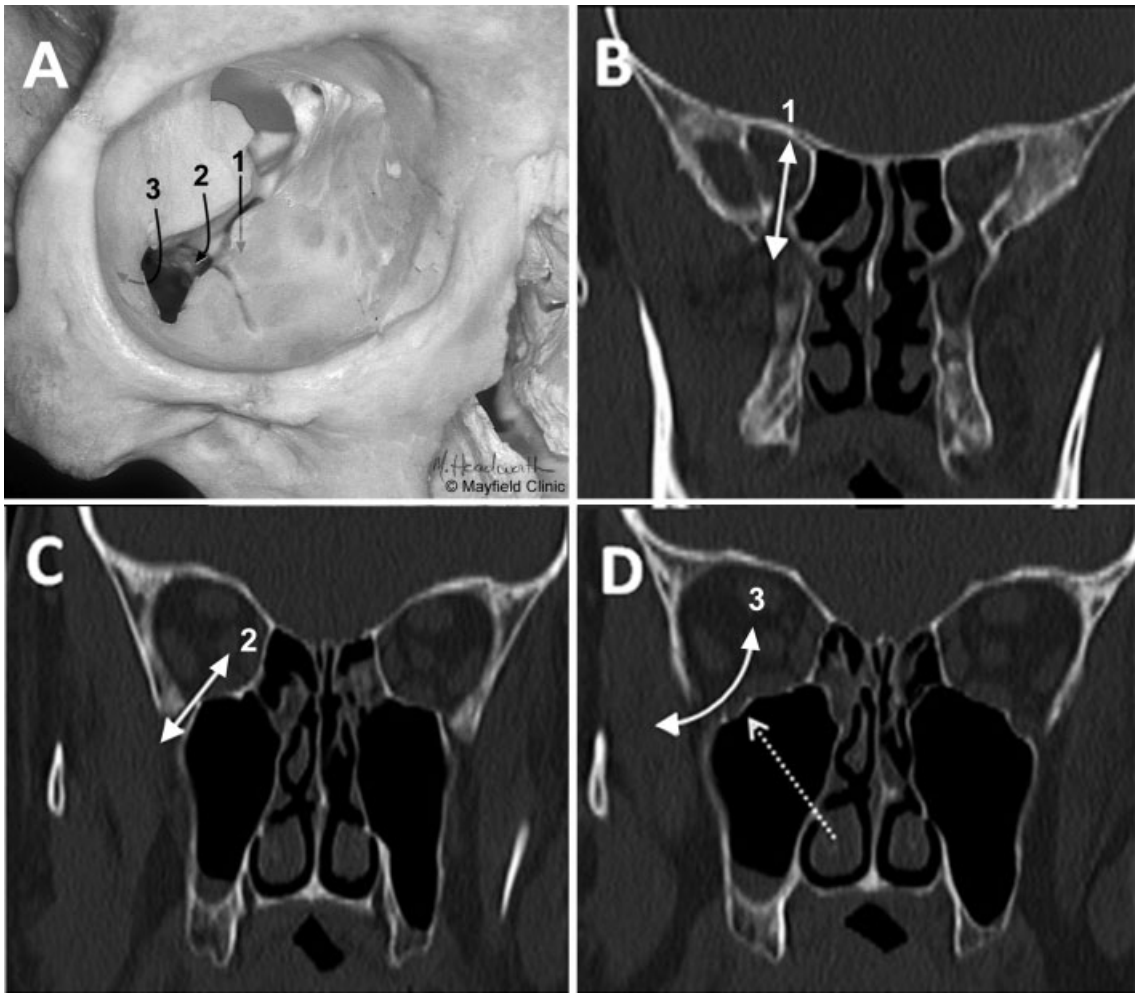

Figure 2 Photograph of the right orbit illustrates communications to various fossae via the three segments of the inferior orbital fissure (IOF): (A) Dry skull photograph of the bony vault of the right orbit. 1 = Posteromedial segment communication with the pterygopalatine fossa. 2 = Middle segment communication with the infratemporal fossa. 3 = Anterolateral segment communication with the temporal fossa. (B) Coronal computed tomography (CT) image through the posteromedial segment of the IOF. Arrow demonstrates communication with the pterygopalatine fossa. (C) Coronal CT image through the middle segment of the IOF. Arrow demonstrates communication in the region of the infratemporal fossa. (D) Coronal CT image through the anterolateral segment of the IOF. Arrow demonstrates communication with the temporal fossa. Note separation of this segment from the infraorbital nerve (arrow with dashed line). (Printed with permission from Mayfield Clinic).

Cadaveric Study

The three approaches to expose the IOF included a total maxillary antrostomy and ethmoidectomy, an endoscopic-modified medial maxillectomy, and a combined endoscopic-modified medial maxillectomy and Caldwell-Luc approach. In the first approach, a large maxillary antrostomy and anterior and posterior ethmoidectomy were performed allowing identification of the maxillary ostium, lamina papyracea, sphenopalatine artery, and posterior nasal artery. The posterior wall of maxillary antrum and the ascending process of the palatine bone were removed using Kerrison rongeurs providing access to the pterygopalatine fossa. Removal of fat from this fossa exposed the sphenopalatine ganglion, vidian nerve, infraorbital nerve, and branches of the maxillary nerve

Table 1 Morphometric Analysis in 50 Dry Cadaveric Skulls (100 Slides)

Skulls	Length/ Width (mm)			
	Anterolateral	Middle	Posteromedial	Total
Average	6.5/5	5.0/3.2	17.0/2.4	29.1
Maximum	11.0/8.7	10.0/6.0	22.0/4.2	35.0
Minimum	3.0/1.9	3.0/1.0	13.0/1.2	23.0

Highlighting the length and width of the three segments of the inferior orbital fissure.

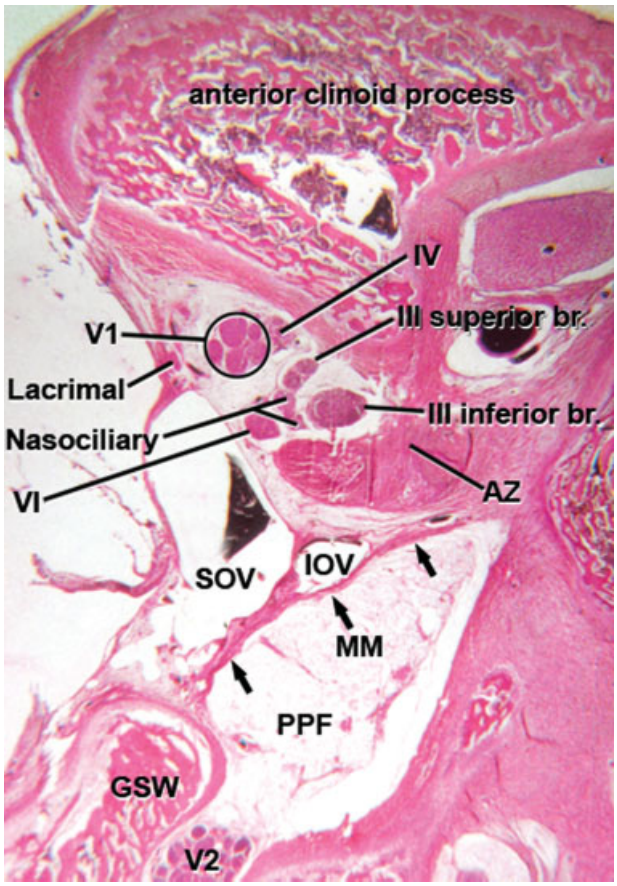

Figure 3 Coronal histological section (100×) of the orbit/orbital apex and at the level of the posteromedial segment (stained with hematoxylin and eosin). Muller's muscle (MM) forms the roof of the pterygopalatine fossa (PPF). Also identified are the medial aspect of the greater wing of the sphenoid (GSW) and the second branch of the trigeminal nerve (V2) coursing to the foramen rotundum, and the relationship of MM to the inferior ophthalmic vein (IOV) near the anterior confluence. Note where the superior ophthalmic vein (SOV) and IOV join and enter the anterior aspect of the cavernous sinus, and the course of MM inferior to the annulus of Zinn (AZ). (Printed with permission from The Institute of Anatomy, College of Medicine, University of Strasbourg).

(V2) posterior to the internal maxillary artery. The maxillary nerve was followed in a retrograde direction to the maxillary strut exposing the posteromedial segment of the IOF.

By histological examination, smooth muscle was identified along the entire extent of the IOF. The muscle was intimately associated with V2 from the foramen rotundum to the infraorbital groove where the two structures diverge; V2 abruptly courses anteromedially while the muscle continues anterolaterally in the IOF. Muller's muscle overlies V2 in the posteromedial segment. The maxillary antrostomy, total ethmoidectomy approach did not allow visualization of the middle and anterolateral segment of the IOF with 0-degree endoscopy (►**Fig. 4A**).

To allow further access, a modified medial maxillectomy approach preserving the nasolacrimal canal is used to gain additional visualization of the IOF as the posterior two-third of the inferior turbinate is removed using endoscopic scissors and rongeurs. This allows working access to the middle segment of the IOF. Smooth muscle is again identified in the middle segment of the IOF; this muscle is above V2 in the posteromedial segment and serves in the middle segment as a roof of the infraorbital groove (►**Fig. 4B**).

With addition of a Caldwell-Luc approach to allow exposure of the anterolateral segment of the IOF, a sublabial incision is made under the upper lip and an anterior maxillotomy gives access to the maxillary sinus. After opening the anterior wall of the maxillary sinus, the infraorbital nerve and artery and anterolateral portion of the IOF are identified. In the anterolateral segment of the IOF, the muscle is relatively thin, consisting primarily of connective tissue. All three IOF segments are readily identified in the Caldwell-Luc approach (►**Fig. 4C**).

Discussion

Our morphometric, cadaveric, and histologic evaluations of the anatomy of the IOF better defined the relationship of this structure to surrounding skull base foraminae and fossae, thus establishing its importance as a landmark for endoscopic cranial base surgery. Furthermore, our classification of the IOF into three segments—specifically the posteromedial, middle, and anterolateral segments–provides distinctive landmarks to the foraminae and fossae of the anterolateral skull base.

Anatomical Considerations

The IOF is formed posterolaterally by the greater wing of the sphenoid bone, laterally by the zygomatic bone, medially by the sphenoid body and a short segment the palatine bone, and anteriorly by the maxilla. This fissure lies along the inferolateral angle of the orbit, and separates the lateral wall from the floor in their posterior two-thirds. It is bound above by the inferior margin of the greater wing of sphenoid bone, and below by the lateral margins of the orbital surface of palatine bone behind and that of maxilla in front. Posteriorly, the foramen rotundum opens into it; just above this point, it continues with the lower end of the superior orbital fissure. The IOF is narrower in the center than at the extremities, wide in its anterior end, and is completed by the zygomatic bone.

In two earlier studies, the IOF was divided into anterolateral, middle, and posteromedial segments.[28,31] The first segment, the anterolateral portion of the fissure, communicates with the temporal fossa inferiorly. In our study, the mean length and width of this portion was 6.5 and 5 mm, respectively; these measurements concur with an earlier study by Lang.[34]

The middle portion of the IOF connects the orbit to the infratemporal fossa. This segment contains the entrance of the infraorbital nerve and artery into the infraorbital groove as described by Rahman et al.[35] Access to the infratemporal fossa is immediately lateral to the infraorbital nerve whereas the pterygopalatine fossa is medial. Indeed, the infraorbital groove or canal is in intimate relationship with the pterygomaxillary fissure, through which the pterygopalatine fossa and infratemporal fossa communicate.[36] Below the middle segment of the IOF are the lateral pterygopalatine muscle and internal maxillary artery. The mean length and width of this

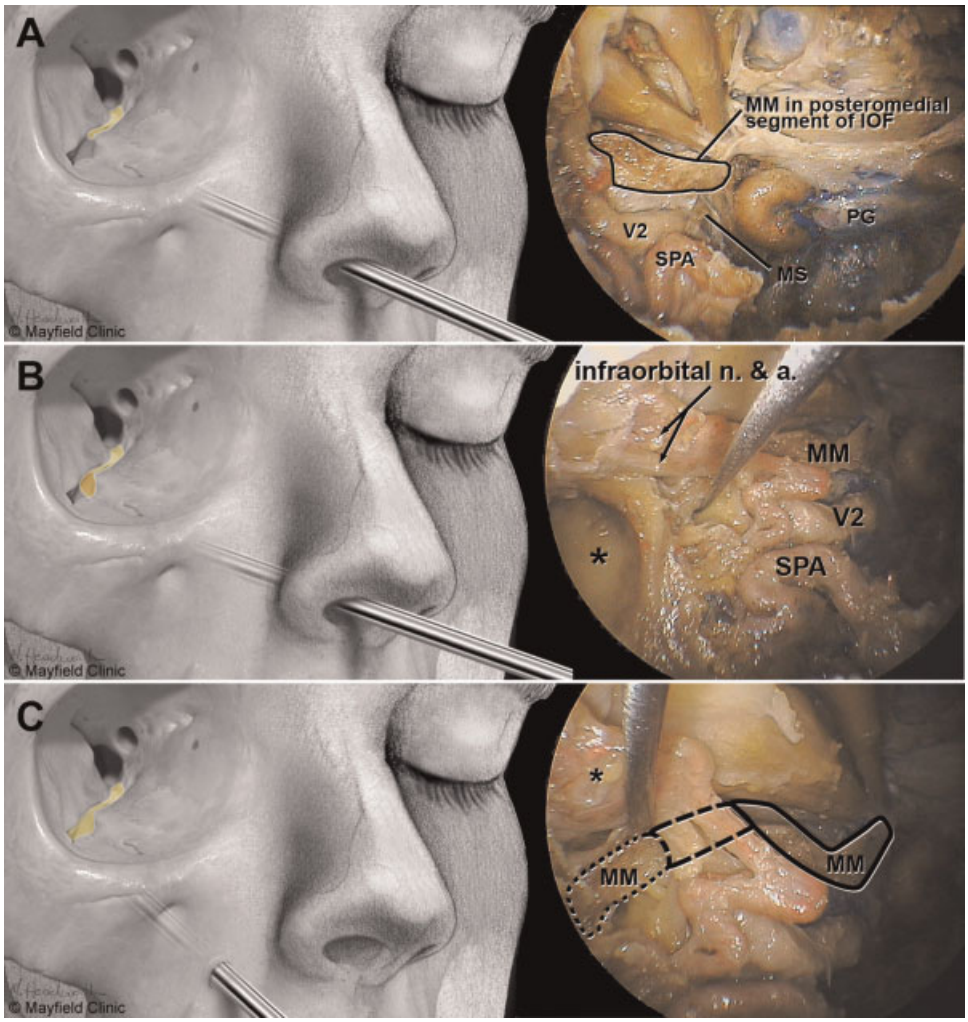

Figure 4 Endoscopic views of cadaveric dissections of the right inferior orbital fissure (IOF) and illustrations depict endscope placement and the corresponding three IOF segments (anterolateral, middle, posteromedial) for each view. (A) Endoscopic anatomy of the posteriomedial segment of the IOF via the maxillary antrostomy, total ethmoidectomy approach. (B) Endoscopic anatomy of the middle and posteromedial segments of the IOF via the combined maxillary antrostomy, total ethmoidectomy, and modified medial maxillectomy approaches (* maxillary sinus). (C) Endoscopic anatomy shows the three segments of the IOF via the combined maxillary antrostomy, total ethmoidectomy, modified medial maxillectomy, and Caldwell-Luc approaches. *infraorbital nerve and artery in the infraorbital groove medial to the IOF. Solid line = posteromedial segment, dashed line = middle segment, dotted line = anterolateral segment. (Printed with permission from Mayfield Clinic.). MM, Mueller's muscle; MS, maxillary strut; PG, pituitary gland; SPA, sphenopalatine artery; V2, second branch of the trigeminal nerve.

portion of the IOF are 5.0 and 3.2 mm, respectively; these measurements differ from 4 mm and 1.5 to 2 mm, respectively, reported earlier by Whitnall.[37] We speculate that this difference might be owing to our larger numbers or ages of specimens (i.e., adult).

The posteromedial portion of the IOF lies above the foramen rotundum and opens into the pterygopalatine fossa. Inferior to this segment are the internal maxillary artery and pterygopalatine ganglion.[38] The second division of the trigeminal nerve (V2) overlies this part of the IOF and gives rise to the infraorbital nerve. The extracranial length of V2 averaged 18 mm (16 to 21 mm) in a report by Herzellah and 17.6 mm (13 to 22 mm) in our morphometric study.[18]

Using histologic examination, we noted that Muller's muscle coursed the entire length of the IOF. First described in 1858 by Müller, it was later called the musculus orbitalis, periorbital muscle, or Muller's muscle.[33,37,39,40] This muscle is part of the orbital connective tissue system and represents an evolutionary vestige from earlier mammalian history.[37,41] Whitnall suggests that Muller's muscle serves both as an accessory muscle for lacrimal function and for protruding the eye in mammals.[37] It forms a bridge over the IOF and separates the orbit from the pterygopalatine fossa, infratemporal fossa, and temporal fossa. In human fetuses, this muscle was consistently present and occupied a large part of the posteroinferior wall of the orbital cavity. Muller's muscle is surrounded by a thin, fascial periosteal sheath that covers the bone of the IOF.

Muller's muscle extends from the inferior part of the cavernous sinus cranially, has an intimate relationship with the annulus of Zinn, reaching the zygomatic and maxillary bone caudally. This important landmark marks where the IOF and SOF join the cavernous sinus. The superior surface of

Muller's muscle is associated with the orbital contents, especially the inferior rectus muscle, the inferior branch of the oculomotor nerve, and the inferior ophthalmic vein and its tributaries. The inferior surface of the muscle is associated with the pterygopalatine fossa and its contents, primarily the maxillary, zygomatic, and infraorbital nerves, which are all surrounded by adipose connective tissue.

Surgical Considerations

Recent reports have shown the capability of the endonasal, endoscopic approaches to access the infratemporal fossa, pterygopalatine fossa, orbit, and cavernous sinus.[4,13–17,23,36] Common pathologies in this region include extensive juvenile nasopharyngeal angiofibromas that involve the pterygopalatine and infratemporal fossae, trigeminal schwannomas, meningiomas that extend extracranially into the infratemporal fossa via the foramen ovale, and adenomas that involve the parasellar cavernous sinus[22–25,42] Although the authors reported adequate removal of tumor, they did not detail the anatomy essential to these approaches.

As mentioned previously, the anterolateral third of the IOF has been used extensively as a landmark for open skull base surgery. In our morphometric and histological studies, the IOF was a landmark for endoscopic approaches to the anterolateral skull base. The three segments, as described previously, led to distinct foraminae and fossae within the skull base. With this knowledge, we compared three endoscopic approaches including the endoscopic maxillary antrostomy and total ethmoidectomy, modified medial maxillectomy, and Caldwell-Luc approaches for access to the segments of the IOF.

The maxillary antrostomy-total ethmoidectomy approach allowed access to the posterior segment of the IOF. Consistent with the histological and morphometric studies, this approach comfortably achieved access to the foramen rotundum and pterygopalatine fossa. Addition of the modified endoscopic medial maxillectomy enabled visualization of the middle and anterolateral segments of the IOF; this modification permitted additional access to the pterygomaxillary fissure and infratemporal fossa described earlier.[43] Previous studies have shown that access to the infratemporal fossa can be achieved with a combined maxillary antrostomy and Caldwell Luc approach.[44] Addition of the Caldwell-Luc approach enhances visualization of the anterolateral segment of the IOF and access to the temporal fossa, frontotemporal skull base, and zygomatic arch. With knowledge of the fossae and foraminae involved with tumor, endoscopic approaches can be tailored to achieve the exposure needed for complete visualization and removal of tumor. A keen anatomical understanding of the IOF and surrounding areas enables one to surgically approach these tumors with the necessary endoscopic visualization and exposure.

Conclusion

Our examination of the morphometric and histological anatomy of the IOF led to its classification into three segments relative to the infraorbital nerve and fossae, each adjacent to a distinctive part of the IOF. In our cadaveric dissections, we could match the specific segment of the IOF with a surgical approach, thus confirming the IOF an important landmark for endonasal endoscopic surgery of the skull base. Knowledge of its anatomy can help both neurosurgeons and otolaryngologists who navigate in the region.

References

1 Al-Nashar IS, Carrau RL, Herrera A, Snyderman CH. Endoscopic transnasal transpterygopalatine fossa approach to the lateral recess of the sphenoid sinus. Laryngoscope 2004;114(3):528–532
2 Anand VK, Schwartz TH, eds. The endoscopic, transsphenoidal, transplanum, transtuberculum approach to the suprasellar cistern. In: Anand VK, Schwartz THeds. Practical Endoscopic Skull Base Surgery. San Diego: Plural Publishing; 2007105–122
3 Burkart CM, Theodosopoulos PV, Keller JT, Zimmer LA. Endoscopic transnasal approach to the clivus: a radiographic anatomical study. Laryngoscope 2009;119(9):1672–1678
4 Cavallo LM, Cappabianca P, Galzio R, Iaconetta G, de Divitiis E, Tschabitscher M. Endoscopic transnasal approach to the cavernous sinus versus transcranial route: anatomic study. Neurosurgery 2005; 56(2, Suppl):379–389, discussion 379–389
5 Cavallo LM, Messina A, Gardner P, et al. Extended endoscopic endonasal approach to the pterygopalatine fossa: anatomical study and clinical considerations. Neurosurg Focus 2005;19(1):E5
6 de Divitiis E, Cappabianca P, Cavallo LM. Endoscopic transsphenoidal approach: adaptability of the procedure to different sellar lesions. Neurosurgery 2002;51(3):699–705, discussion 705–707
7 Jho HD, Ha HG. Endoscopic endonasal skull base surgery: Part 1—The midline anterior fossa skull base. Minim Invasive Neurosurg 2004;47(1):1–8
8 Kassam AB, Gardner P, Snyderman C, Mintz A, Carrau R. Expanded endonasal approach: fully endoscopic, completely transnasal approach to the middle third of the clivus, petrous bone, middle cranial fossa, and infratemporal fossa. Neurosurg Focus 2005;19 (1):E6
9 Kassam AB, Snyderman C, Gardner P, Carrau R, Spiro R. The expanded endonasal approach: a fully endoscopic transnasal approach and resection of the odontoid process: technical case report. Neurosurgery 2005;57(1, Suppl):E213, discussion E213
10 Laufer I, Anand VK, Schwartz TH. Endoscopic, endonasal extended transsphenoidal, transplanum transtuberculum approach for resection of suprasellar lesions. J Neurosurg 2007;106(3):400–406
11 Schwartz TH, Fraser JF, Brown S, Tabaee A, Kacker A, Anand VK. Endoscopic cranial base surgery: classification of operative approaches. Neurosurgery 2008;62(5):991–1002, discussion 1002–1005
12 Stamm AC, Pignatari SS, Vellutini E. Transnasal endoscopic surgical approaches to the clivus. Otolaryngol Clin North Am 2006;39 (3):639–656, xi
13 Alfieri A, Jho HD, Schettino R, Tschabitscher M. Endoscopic endonasal approach to the pterygopalatine fossa: anatomic study. Neurosurgery 2003;52(2):374–378, discussion 378–380
14 Fortes FS, Sennes LU, Carrau RL, et al. Endoscopic anatomy of the pterygopalatine fossa and the transpterygoid approach: development of a surgical instruction model. Laryngoscope 2008;118 (1):44–49
15 Magro F, Solari D, Cavallo LM, et al. The Endoscopic endonasal approach to the lateral recess of the sphenoid sinus via the petrygopalaitine fossa; Comparison of endoscopic and radiological landmarks. Neurosurgery 2006;59(suppl 4):ONS-237–ONS-243
16 Gönül E, Erdogan E, Düz B, Timurkaynak E. Transmaxillary approach to the orbit: an anatomic study. Neurosurgery 2003;53 (4):935–941, discussion 941–942

17 Har-El G. Combined endoscopic transmaxillary-transnasal approach to the pterygoid region, lateral sphenoid sinus, and retrobulbar orbit. Ann Otol Rhinol Laryngol 2005;114(6):439–442
18 Herzallah IR, Elsheikh EM, Casiano RR. Endoscopic endonasal study of the maxillary nerve: a new orientation. Am J Rhinol 2007;21(5):637–643
19 Kamel RH. Transnasal endoscopic surgery in juvenile nasopharyngeal angiofibroma. J Laryngol Otol 1996;110;962–968
20 Cavallo LM, Messina A, Gardner P, et al. Extended endoscopic endonasal approach to the pterygopalatine fossa: anatomical study and clinical considerations. Neurosurg Focus 2005;19(1):E5
21 Ong BC, Gore PA, Donnellan MB, Kertesz T, Teo C. Endoscopic sublabial transmaxillary approach to the rostral middle fossa. Neurosurgery 2008;62(3, Suppl 1):30–36, discussion 37
22 Jian XC, Wang CX, Jiang CH. Surgical management of primary and secondary tumors in the pterygopalatine fossa. Otolaryngol Head Neck Surg 2005;132(1):90–94
23 Martínez Ferreras A, Rodrigo Tapia JP, Llorente Pendás JL, Suárez Nieto C. [Endoscopic nasal surgery for pterigopalatine fossa schwannoma]. Acta Otorrinolaringol Esp 2005;56(1):41–43
24 Kafadar AM, Tanriverdi T, Canbaz B, Kuday C. Trigeminal neuroma with extracranial extension: the 31st case. Minim Invasive Neurosurg 2006;49(4):230–233
25 Kamel RH. Transnasal endoscopic surgery in juvenile nasopharyngeal angiofibroma. J Laryngol Otol 1996;110(10):962–968
26 Teresi LM, Lufkin RB, Viñuela F, et al. MR imaging of the nasopharynx and floor of the middle cranial fossa. Part II. Malignant tumors. Radiology 1987;164(3):817–821
27 Yu Q, Wang P, Shi H, Luo J, Sun D. The lesions of the pterygopalatine and infratemporal spaces: Computed tomography evaluation. Oral Surg Oral Med Oral Pathol Oral Radiol Endod 1998;85(6):742–751
28 Aziz KM, Froelich SC, Cohen PL, Sanan A, Keller JT, van Loveren HR. The one-piece orbitozygomatic approach: the MacCarty burr hole and the inferior orbital fissure as keys to technique and application. Acta Neurochir (Wien) 2002;144(1):15–24
29 Hakuba A, Liu S, Nishimura S. The orbitozygomatic infratemporal approach: a new surgical technique. Surg Neurol 1986;26(3):271–276
30 Martins C, Li X, Rhoton AL Jr. Role of the zygomaticofacial foramen in the orbitozygomatic craniotomy: anatomic report. Neurosurgery 2003;53(1):168–172, discussion 172–173
31 Shimizu S, Tanriover N, Rhoton AL Jr, Yoshioka N, Fujii K. MacCarty keyhole and inferior orbital fissure in orbitozygomatic craniotomy. Neurosurgery 2005;57(1, Suppl):152–159, discussion 152–159
32 Sanan A, Abdel Aziz KM, Janjua RM, van Loveren HR, Keller JT. Colored silicone injection for use in neurosurgical dissections: anatomic technical note. Neurosurgery 1999;45(5):1267–1271, discussion 1271–1274
33 Müller H. Über einen glatten Muskel in der Augenhöhle des Menschen und der Säugetiere. Z wis Zool 1858;9;541
34 Lang J. Clinical Anatomy of the Head, Neurocranium, Orbit, and Craniocervial Regions. Springer Verlag; 1983
35 Rahman M, Richter EO, Osawa S, Rhoton AL Jr. Anatomic study of the infraorbital foramen for radiofrequency neurotomy of the infraorbital nerve. Neurosurgery 2009;64(5, Suppl 2):423–427, discussion 427–428
36 Zimmer LA, Hart C, Theodosopoulos PV. Endoscopic anatomy of the petrous segment of the internal carotid artery. Am J Rhinol Allergy 2009;23(2):192–196
37 Whitnall SE. Part I Osteology. The bone forming the orbit, its relations, and the accessory air-sinuses of the nose. The anatomy of the human orbit and accessory organs of vision. 2nd ed. Oxford University Press; 193241–43, 86–89
38 Choi J, Park HS. The clinical anatomy of the maxillary artery in the pterygopalatine fossa. J Oral Maxillofac Surg 2003;61(1):72–78
39 Rodríguez Vázquez JF, Mérida Velasco JR, Jiménez Collado J. Orbital muscle of Müller: observations on human fetuses measuring 35-150 mm. Acta Anat (Basel) 1990;139(4):300–303
40 Rodríguez-Vázquez JF, Mérida-Velasco JR, Arráez-Aybar LA, Jiménez-Collado J. Anatomic relationships of the orbital muscle of Müller in human fetuses. Surg Radiol Anat 1998;20(5):341–344
41 Dutton JJ. Atlas of Clinical and Surgical Orbital Anatomy. Philadelphia: Saunders; 1994:100–101
42 Waitz G, Wigand ME. Results of endoscopic sinus surgery for the treatment of inverted papillomas. Laryngoscope 1992;102(8): 917–922
43 Zimmer LA, Theodosopoulos PV. Anterior skull base surgery: open versus endoscopic. Curr Opin Otolaryngol Head Neck Surg 2009;17(2):75–78
44 Theodosopoulos PV, Guthikonda B, Brescia A, Keller JT, Zimmer LA. Endoscopic approach to the infratemporal fossa: anatomic study. Neurosurgery 2010;66(1):196–202, discussion 202–203